Biophysical Journal Volume 72 April 1997 1842–1848

Two-Dimensional Arrangement of a Functional Protein by Cysteine-Gold Interaction: Enzyme Activity and Characterization of a Protein Monolayer on a Gold Substrate

Yuji C. Sasaki,* Kenji Yasuda,* Yoshio Suzuki,* Tadashi Ishibashi,* Isamu Satoh,# Yasutake Fujiki,§ and Shin'ichi Ishiwata§¶

*Advanced Research Laboratory, Hitachi Ltd., Saitama 350-03, Japan; #Institute for Materials Research, Tohoku University, Sendai 980-77; and §Department of Physics, School of Science and Engineering, and ¶Advanced Research Institute for Science and Engineering, Waseda University, Tokyo 169, Japan

ABSTRACT We have characterized the functional protein, myosin subfragment 1 (S1), attached to a gold substrate by the sulfhydryl groups of cysteine in proteins. The amino groups of the regulatory light chain (RLC) isolated from myosin were labeled with a radioisotope (^{125}I), and the labeled RLC was incorporated into S1 from which the RLC had been removed. The radiation from ^{125}I showed that S1 molecules had attached to the gold and, through the interference effect of the monochromatic radiation from ^{125}I, provided information about the position of labeled RLC sites in the S1 monolayer. The interference fringes showed that the RLC was located close to the gold surface and that all of the adsorbed S1 molecules had the same orientation. We confirmed that the motor function of S1 on the gold surface is maintained by observing sliding movement at low ionic strength and by observing the detachment at high ionic strength of fluorescent actin filaments in the presence of ATP. We also found that the adsorbed S1 molecules were not removed from the Au surface by a reducing agent. Thus the Au-S bond is more stable than the S-S bond.

INTRODUCTION

A two-dimensional arrangement of molecules on a gold surface has recently been investigated through the adsorption of long-chain organic thiols; these thiols formed well-ordered monolayers of molecules by self-assembly driven by the formation of stable gold-sulfide (Au-S) bonds and van der Waals interactions between the side chains of the molecules (Whitesides and Laibinis, 1990). This technique of forming self-assembled monolayers can be used to create new kinds of functionalized surfaces that are suitable, for example, for molecular recognition, which is an essential biological phenomenon.

Two-dimensional arrangements have also been formed when protein molecules were electrostatically adsorbed to a positively charged Langmuir-Blodgett (LB) film (Sasaki et al., 1993, 1994a; Caffrey and Wang, 1995) and hydrophobically adsorbed to a nitrocellulose-coated surface (Kron et al., 1991; Suzuki et al., 1996), a silicone-treated surface (Harada et al., 1990), or a hexamethyldisilazane (HMDS)-treated surface (Nishizaka et al., 1995). Two-dimensional arrangements of protein molecules have also been formed by allowing the molecules to adsorb onto biotin-containing bioreactive surfaces (Muller et al., 1993). These techniques cannot, however, provide protein molecules that have the same orientation, and they are highly dependent on the quality of the modified surfaces. Although organofunctional silane coupling agents on the glass surface also have been successfully used to improve the chemisorption on the surface, the functional sites at the ends of silane coupling agent are also found to interact with the silica surface (Moses et al., 1978; Chiang et al., 1980). Thus the efficiency of the reaction between the proteins and the functional sites is very low.

In the work described in this report, we have characterized the arrangement and enzymatic activity of a functional protein adsorbed onto a gold substrate by direct attachment of the sulfhydryl (SH) groups of cysteine in the protein. This adsorption technique was used because of the stable Au-S reaction between the Au surface, which is an atomically flat and clean single Au surface (Hallmark et al., 1987), and the SH group of cysteine, which is highly reactive, in the protein.

We have chosen myosin molecules as an enzyme that appears to be suitable for applying this technique, because large conformational changes are expected. Myosin is an asymmetrical molecule of about 480 kDa, and it consists of two heavy chains and four light chains. Myosin molecules can be digested into two parts by limited proteolysis with papain: two subfragments, about 130 kDa each (called S1), and one rod-shaped fragment (called myosin rod), with a molecular mass of about 220 kDa. A pair of light chains with molecular masses between 15 and 22 kDa (an essential light chain (ELC) and a regulatory light chain (RLC)), are associated with each S1 molecule. In an in vitro motility assay recently invented to observe the mechano-chemical coupling of molecular motors such as myosin and kinesin, motor molecules are usually bound to a hydrophobic surface on a glass slide. With these methods it is difficult, however, to control the orientation of the motor molecules in this assay, because they have many hydrophobic sites.

Received for publication 3 June 1996 and in final form 8 January 1997.

Address reprint requests to Dr. Yuji C. Sasaki, Advanced Research Laboratory, Hitachi Ltd., Hatoyama, Saitama 350–03, Japan. Tel.: 81-492-96-6111; Fax: 81-492-96-6006; E-mail: ycsasaki@harl.hitachi.co.jp.

0006-3495/97/04/1842/07 $2.00

There have recently been several reports of attempts to arrange motor molecules at a fixed orientation on a glass surface, for example, with the use of specific binding of an avidin-biotin system (Itakura et al., 1993). The direct attachment to a gold surface through the SH group in a certain cysteine residue of a protein is an alternative and powerful technique for arranging the proteins in a vertical direction. The technique of interference pattern from radioisotopes (IPR) can be used to determine the position of a specific site of arranged proteins to which radioisotopes are incorporated (Sasaki et al., 1994a). In the present approach, the vertical movement of the two-dimensionally arranged myosin monolayer may be observed if the conformational changes of myosin molecules occur because of changes in environmental conditions.

MATERIALS AND METHODS

Preparation of the specifically labeled S1 molecules

Myosin prepared from rabbit skeletal white muscle was digested with papain in the presence of Mg^{2+} at 25°C for 8 min to obtain S1, which was purified by high-performance gel filtration (Superose 6; Pharmacia, Piscataway, NJ) (Kron et al., 1991). The regulatory light chain (RLC) was isolated by treating the myosin with 5,5′-dithiobis(2-nitrobenzoic acid) for 10 min at 4°C (Wagner, 1982). The isolated RLC (1.13 mg/ml) was labeled with di[^{125}I]-Bolton-Hunter (BH) reagent (Dupont, DE), which was reacted with amino groups in the protein molecules, in a 5 mM phosphate buffer (pH 8.0) for 1 h at 25°C (Bolton and Hunter, 1973). The isolated RLC (5.1×10^{-10} mole) was labeled with di[^{125}I]-BH reagent (8.0×10^{-11} mole). The ratio between the number of the RLC molecules and radioisotope reagent was approximately 6:1. After ultrafiltration, we confirmed that the ratio between the number of the RLC molecules and labeled radioisotopic reagent was approximately 12:1. On average, about one ^{125}I was incorporated into 12 RLC molecules. The radiolabeled RLC was incubated for 5 min at 25°C in a rigor solution (RS) (0.1 M KCl, 5 mM $MgCl_2$, and 10 mM 3-(*N*-morpholino)propanesulfonic acid; pH 7.0) containing 1 mM thimerosal (mercury-[(*o*-carboxyphenyl)thio]ethyl sodium salt; Sigma Chemical Co., St. Louis, MO), an SH reagent, to block the SH groups (Emoto et al., 1985). After the free thimerosal was removed, the thimerosal-labeled RLC was mixed with S1 from which the RLC had been removed in an EDTA solution (ES) (50 mM KCl, 20 mM EDTA, and 20 mM 3-(*N*-morpholino)propanesulfonic acid, pH 7.0), and was incubated for 2 h at 4°C. The S1 molecules containing the radioiodinated and thimerosal-labeled RLC were incubated on a Au substrate overnight at 4°C in RS and then washed with RS to remove the excess S1.

Preparation of S1 molecules

To check the direct reaction of the Au-S bonds between the gold surface and the S1 molecules, we examined four different preparations of S1: 1) untreated S1(S1); 2) S1 in which the SH groups of the RLC had been modified with thimerosal (S1*); 3) S1, all all the SH groups of which had been modified with thimerosal (S1**); and 4) S1, the most reactive SH group (Cys707 in the heavy chain called SH1) of which had been labeled with 5-eosinylmaleimide (EMI) ($S1^+$). The S1* was prepared as described above. The S1** was prepared by incubating untreated S1 (0.43 mg/ml) in RS containing 1 mM thimerosal for 5 min at 25°C. Four to five SH groups of S1 are thought to be labeled with thimerosal (Emoto et al., 1985). The $S1^+$ was prepared according to the method of Kinosita et al. (1984). The S1, S1*, S1**, and $S1^+$ thus obtained were labeled with di[^{125}I]-Bolton-Hunter reagent in 5 mM phosphate buffer (pH 8.0) for 1 h at 25°C to obtain the radiated S1, S1*, S1**, and $S1^+$, respectively. The radiolabeled S1, S1*, S1**, and $S1^+$ preparations were separately incubated on gold substrates overnight at 4°C in RS and then washed with RS to remove the excess S1s. We found that the S1 molecules did not adsorb to the gold substrate in the buffer containing the reduced form of glutathione, β-mercaptoethanol, or dithiothreitol (DTT) (data not shown). These SH reductants might have prevented the reaction between the S1 and Au surface and therefore were not included in the buffer used when the S1 was bound to the Au surface.

Theory of interference fringes from ^{125}I

This interference effect is generated as a result of the interaction between the direct monochromatic emission from the radioisotopes and the emission totally reflected by the substrate surface (Fig. 1). In other words, it is a Lloyd's-mirror-type interference phenomenon in the x-ray wavelength region (Sasaki et al., 1994b, 1995). Interference fringes can be clearly observed when the take-off angle (θ_t) for electron-capture x-rays emitted from radioisotopes is smaller than the critical angle (θ_c) for x-ray total external reflection. In the theoretical interference pattern from radioisotopes (IPR), we modeled three homogeneous media as stratified media: air, a layer of the myosin S1 molecules labeled with radioactive atoms (^{125}I), and a gold substrate (Fig. 2). Although there is also actually a solution layer and polyimide layer on the sample system, the interference effect of x-rays from ^{125}I is independent of the presence of these solution layers, because their thicknesses (5–7 μm) are greater than the coherence length of the measured electron-capture x-rays. These films only influence the x-ray refraction at each interface. The theoretical IPR from a stratified medium can be obtained on the basis of both the solution of Maxwell's equations for optical electromagnetic waves on each interface and the reciprocity. In other words, the calculation of the x-ray intensity from coordinate z for take-off angle θ_t is identical to that of the incident x-ray field at coordinate z for glancing angle θ_t. When radioactive atoms act as x-ray sources with distribution N, the yield Y is given by

$$I(\theta_t, z) = |E_d + E_r|^2 \tag{1}$$

and

$$Y(\theta_t) = \int N(z) I(\theta_t, z)\, dz, \tag{2}$$

where $I(\theta_t, z)$ is the intensity of x-rays due to interference effects between the direct and totally reflected emissions from coordinate z at the take-off angle (θ_t); E_d and E_r are, respectively, the E-field plane waves of the direct

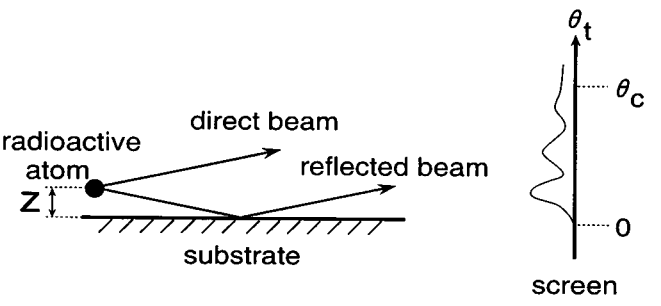

FIGURE 1 Schematic of the interference phenomenon of the electron-capture x-ray from a radioactive atom embedded within a sample. z represents the distance between the radioactive atom and the substrate surface. θ_t is the take-off angle of the electron-capture x-rays. Although emissions from radioisotopes have the form of a spherical wave, a plane wave, which is one of the components of a spherical wave, is observed under the conditions of this experiment. This is because the distance between the observation point and the atomic source points is very long.

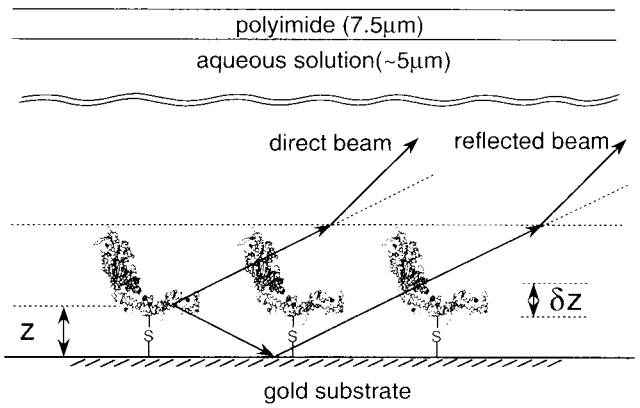

FIGURE 2 Schematic of the cross-sectional view of an ^{125}I-labeled myosin S1 monolayer and the interference phenomenon of a monochromatic radiation from ^{125}I. z and δz represent the distance between the ^{125}I atoms and the substrate surface and the distribution width of the ^{125}I atoms, respectively. There is a refraction effect at the interface between the aqueous solution layer and the S1 molecule layer. The interference fringes between the direct beam and the reflected beam from ^{125}I atoms are influenced by this refraction effect. Thus we can obtain the information about the position of the interface between the aqueous solution layer and the S1 molecule layer. The illustration of S1 was taken from Rayment et al. (1993), but the location of the SH groups is not necessarily accurate.

and reflected emissions; and $N(z)$ is the distribution of labeled atoms, ^{125}I, at a distance z from the substrate surface. In this work we calculated the theoretical angular distribution by considering the interference effect and the refraction effect at each interface of the solution layer and the polyimide film. Thus we could obtain not only the position of ^{125}I (z), but also the total thickness (in other words, the vertical total width of adsorbed S1 molecules) by considering the refraction effect at the interface between the solution layer and the layer of the S1 molecules. The intensity decay of the electron-capture x-rays was ignored by considering the long radioactive decay rate (the half-life time is 60.1 days), whereas the time taken to obtain one datum was about 24 h. In evaluating the theoretical fringes for the normalized yield, we used the following data for the values of 1 (the complex refractive indices) for Te Kα: $(3.2 + 0.0012\,i) \times 10^{-7}$ for the monolayers of protein S1, and $(5.6 + 0.018\,i) \times 10^{-5}$ for the gold substrate in which i is the imaginary unit. Those values for the complex indices of refraction were determined in the χ^2 minimization fitting of the measured interference fringes.

Instrumentation

Fig. 3 is a schematic drawing of the experimental apparatus we used for IPR measurements. The angular distribution of the electron-capture x-rays was measured by scanning the slit along the transversal direction. A slit (30 μm high and 10 mm wide) was placed before a detector at a distance of 200 mm from the sample to determine the take-off angle (θ_t). The angular distribution of electron-capture x-rays was monitored with an energy-dispersive detector (pure Ge detector; EG&G ORTEC, TN). The angular resolution in the measured region was less than 0.3 mradians. All IPR measurements were carried out at 4°C.

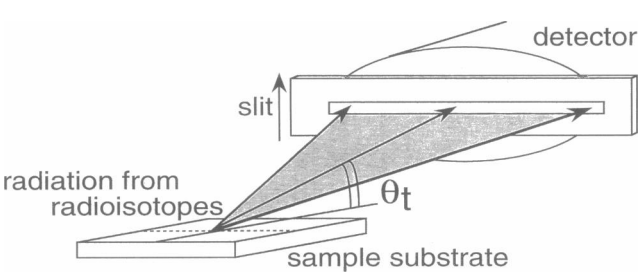

FIGURE 3 Schematic drawing of the experimental apparatus for IPR measurement. The electron-capture x-rays are monitored by a pure Ge detector through a narrow slit.

Fluorescent images of rhodamine-phalloidin-labeled actin filaments

S1 (S1, S1*, or S1**) (2 mg/ml) in RS solution was introduced on both a hexamethyldisilazane (HMDS)-coated glass coverslip and a 100.0-nm-Au-coated glass coverslip. Both of them were used just after the introduction of S1 solution or after the overnight incubation of S1 at 4°C. Just before observation, solution A (25 mM KCl, 25 mM imidazole HCl (pH 7.4), 4 mM $MgCl_2$, 1 mM EGTA, and 10 mM DTT) containing 0.5 mg/ml bovine serum albumin (BSA) was infused into the cell to coat the bare glass surface (Kron et al., 1991). For measuring the attachment of actin filaments to S1 either on the HMDS-coated or Au-coated glass surface, 0.5 μg/ml actin filaments labeled with rhodamine phalloidin in solution A were infused and then washed with solution B (i.e., solution A containing 4.5 mg/ml glucose, 0.2 mg/ml glucose oxydase, and 0.04 mg/ml catalase). The fluorescent images of rhodamine-phalloidin-labeled actin filaments were observed under a fluorescent microscope (Diaphoto-TMD, NCF Fluor ×100 objective lens, NA = 1.3; Nikon, Tokyo) equipped with a SIT camera (C1000–12; Hamamatsu Photonics K. K., Hamamatsu, Japan) and were recorded on videotape. The video data were analyzed by a computer containing a video capture board (Centris 660AV, Apple Inc., CA). To check the enzymatic activity of S1, both the motility of actin filaments on the glass surface and the detachment of actin filaments from S1 were examined at 27 ± 1°C. For the motility, solution B was exchanged for solution C (i.e., solution B containing 1 mM ATP), and the sliding movement of actin filaments was observed. For the detachment, solution C was exchanged for a high-salt solution D (i.e., solution C containing 0.6 M KCl instead of 25 mM KCl), and the disappearance of fluorescent actin filaments was observed.

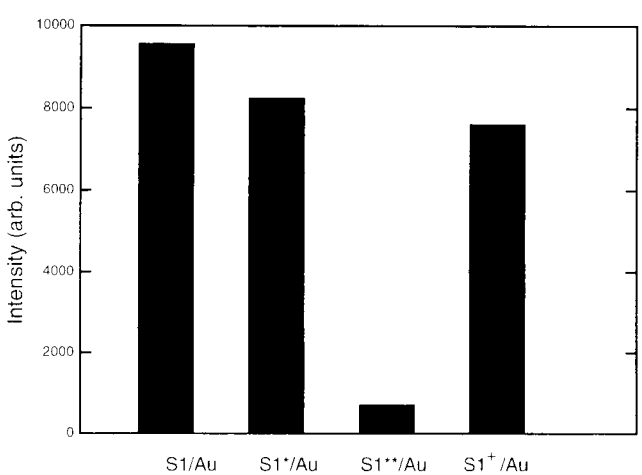

FIGURE 4 Population of ^{125}I-labeled S1 on the gold substrate after adsorption. S1/Au, S1*/Au, S1**/Au, and S1$^+$/Au, respectively, show the population of S1, S1*, S1**, and S1$^+$, the SH1 group of which was labeled with 5-eosinylmaleimide (EMI). The intensity of radiation of the ^{125}I-labeled S1s on the Au substrate was measured by pure Ge detector.

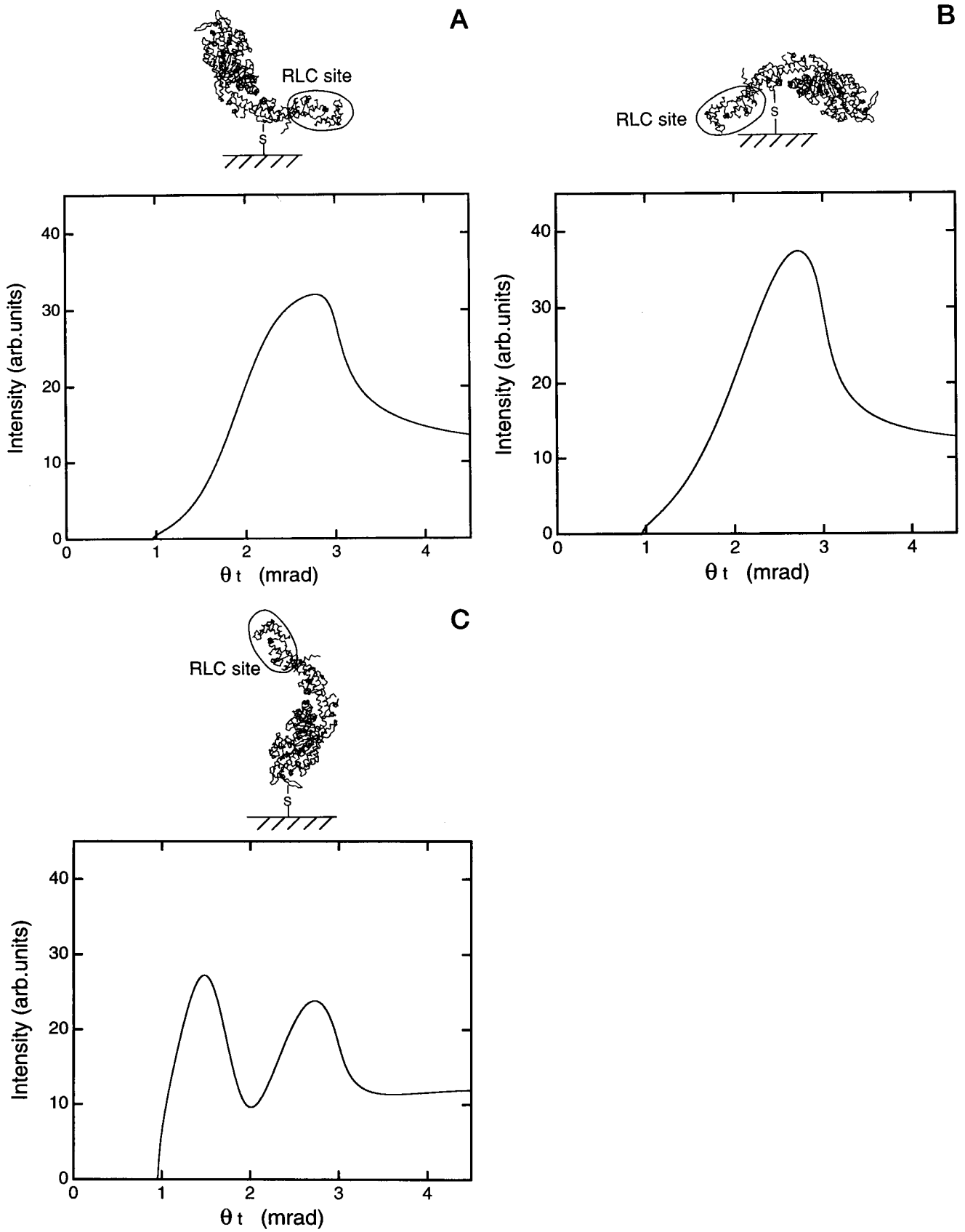

FIGURE 5 The calculated x-ray interference fringes from models *a*, *b*, and *c*. The values of total thickness (t), z_0 and δz for each model were (*a*) t = 10.0 nm, z_0 = 0.5 nm, δz = 1.0 nm; (*b*) t = 7.0 nm, z_0 = 1.0 nm, δz = 1.0 nm; (*c*) t = 14.0 nm, z_0 = 12.0 nm, δz = 3.0 nm. The illustration of S1 was taken from Rayment et al. (1993), but the location of the SH groups is not necessarily accurate.

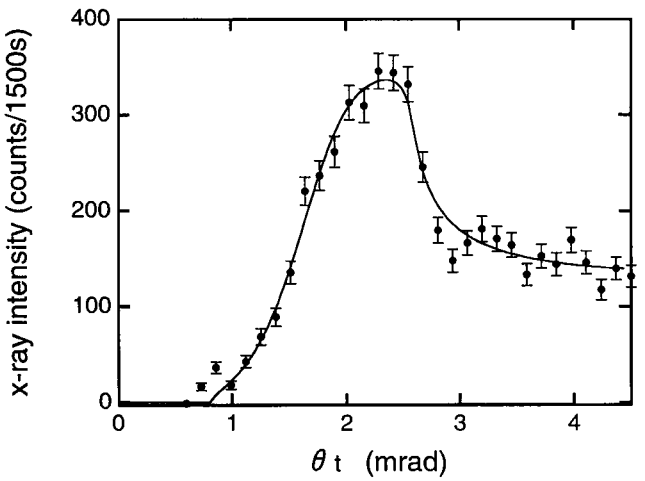

FIGURE 6 The measured angular distribution (*closed circles*) and theoretical one (*line*) of x-ray intensity from ^{125}I. The measured monochromatic radiation is the electron-capture x-rays (Te Kα) from ^{125}I. The statistical error rate for the experimental data was defined by the square root of the number of detected photons.

RESULTS AND DISCUSSION

Adsorption of S1 to a gold surface

First we checked whether the SH groups of the protein could be directly attached to the gold surface by the Au-S bonds. The selectivity in the adsorption of the gold surface was measured by the intensity of radiation from ^{125}I-labeled S1 molecules. Fig. 4 shows that the intensity of radiation from S1** was less than 1/10 of that from untreated S1, whereas that from S1* was nearly equal to that from untreated S1. In addition, we confirmed that SH1 is not the binding site for the Au substrate. These experimental results show that the adsorption of S1 on the gold surface occurs through SH groups other than those of RLC and SH1 of HC.

In additional experiments, we confirmed that the total amount of untreated S1 adsorbed on the Au substrate was approximately equal to that adsorbed on an HMDS-coated glass surface (data not shown). And we checked to see whether the reaction between the S1 and gold surface is the same as the S-S binding reaction. We found that the adsorbed S1 molecules were not removed from the gold surface by the reduced form of the glutathione, β-mercaptoethanol, or DTT. Thus S-Au binding seems to be more stable than S-S binding. These properties were important for the present experiments, because the buffer containing the reductants could be used to avoid the oxidation of the functional proteins adsorbed on the gold substrate.

Arrangement of S1 on a gold surface examined by the IPR method

We used the IPR method to obtain a vertical coordinate of the position of ^{125}I in the S1* monolayer on the Au substrate in an aqueous solution. The IPR method also revealed the vertical distribution of the RLC molecules in the S1* monolayer. The calculated angular distributions of x-ray intensity for assumed orientations of the adsorbed S1* molecules are shown in Fig. 5. In model a, the external SH site of ELC in S1* molecules (for example, Cys136 or Cys177) is directed toward the gold surface. In model b, the SH site of ELC (Cys136 or Cys177) located at the reverse side reacts with the gold surface. In model c the tip of the heavy chain (for example, Cys 402) is attached to the gold surface. In these model calculations we applied the structure of the S1 molecules according to Rayment's 3D structural data (Rayment at el., 1993). The IPRs for models a, b, and c have one and two fringes, respectively. In models a and b, the position of the first fringe peak is shifted to a lower take-off angle when the distance between the radioisotopes and the substrate surface becomes larger. In other words, the period of the calculated fringes is highly dependent on the distance between the radioisotopes and the gold surface. The orientation of the adsorbed S1 molecules can thus be determined by analyzing the interference fringes from the radioisotopes.

As shown in the interference pattern of Te Kα from ^{125}I (Fig. 6), there was one peak at 2–2.5 mradians. Below 0.7 mradians, the intensity of the x-rays could not be measured because of the x-ray refraction at the air-polyimide film interface. We calculated the theoretical interference fringes by χ^2 minimization fitting with Eq. 2. We assumed that $N(z)$ reached a maximum peak at $z = z_0$ and had a Gaussian distribution with a standard deviation σ, because the theoretical fringes are not so influenced by the fine structure of radiolabel distribution. We cannot assign each position of the radiolabeled sites from the experimental IPR when the radiolabeled sites are closer than about 1 nm. We obtained the theoretical curve in Fig. 6, in which a mean ^{125}I position $z_0 = 0.5 \pm 1.9$ nm, a Gaussian distribution width of 2σ (corresponding to δz shown in Fig. 2) $= 1.0 \pm 1.0$ nm, and a total thickness of S1 monolayer $= 10.0 \pm 1.9$ nm. The standard errors of z_0, 2σ, and the total thickness were obtained by χ^2 minimization fitting. Our experimental results indicated that the measured distribution of ^{125}I was Gaussian, with a width 2σ of 1.0 ± 1.0 nm. This value for the distribution of ^{125}I is much smaller than the total thickness (10.0 ± 1.9 nm) of the S1 monolayer. This value is also smaller than the size of RLC (2.4×5.2 nm). This indicates that the RLC sites are located close to the gold surface. We also obtained the position ($= 0.5 \pm 1.9$ nm) of the RLC subunit from the gold surface. The RLC subunit is located in the tail of the heavy chain. Thus we conclude that the orientation of the adsorbed S1 is as shown in model a of Fig. 5.

Considering both the structural data of S1 molecules (Rayment et al., 1993) and the above results, we infer that the binding site for the Au substrate is the cysteine in the α-helix of the heavy chain (Cys815) or in the essential light chain (Cys136 and/or Cys177). The cysteine in the α-helix of the heavy chain might be covered by the essential light chain. It is difficult to identify the binding site for the Au

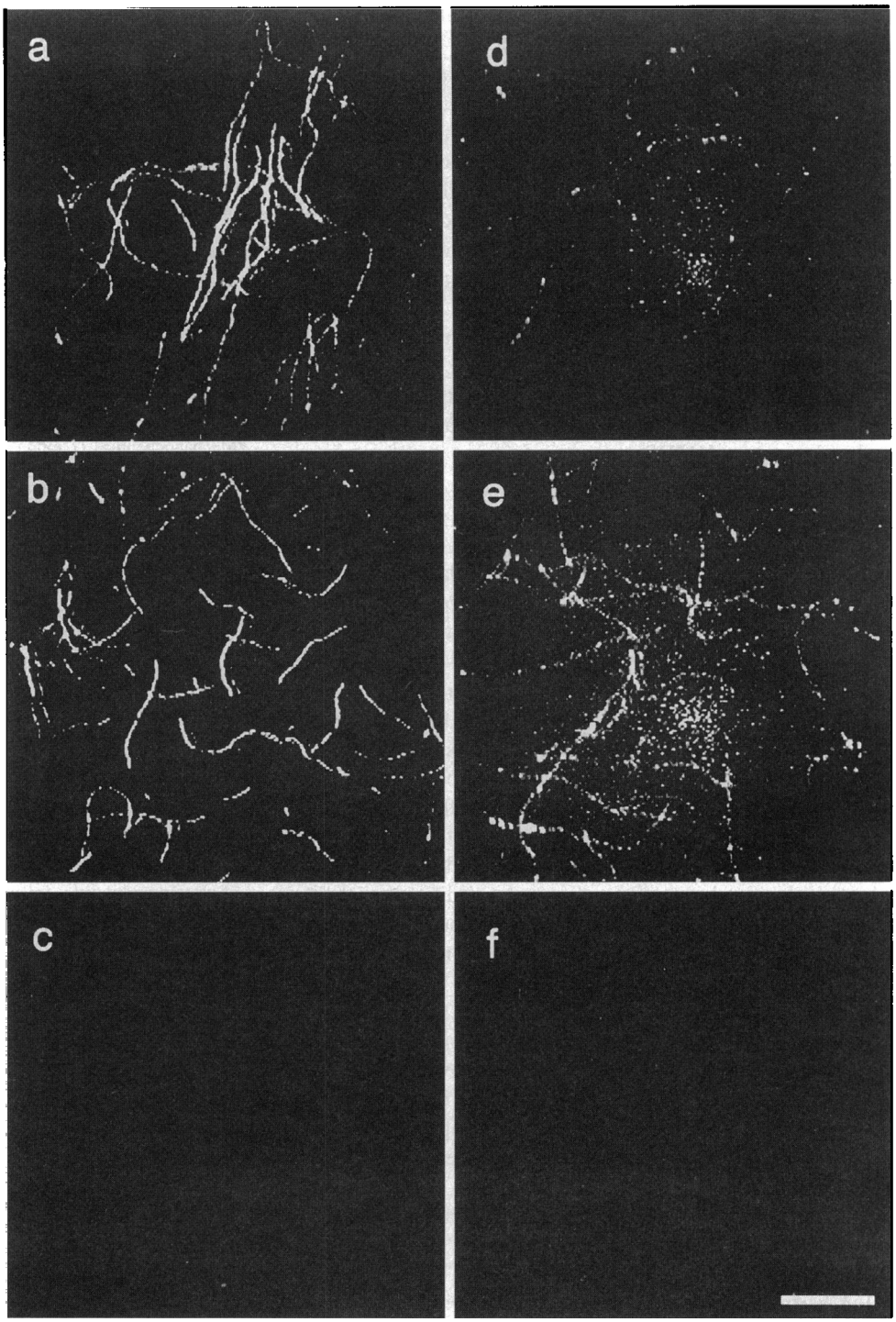

FIGURE 7 Fluorescent images of rhodamine phalloidin-labeled actin filaments. Rhodamine phalloidin-labeled actin filaments (0.5 μg/ml) (25 mM KCl, 25 mM imidazole HCl (pH 7.4), 4 mM $MgCl_2$, 1 mM EGTA, and 1 mM DTT) infused after 0.1 mg/ml S1 were introduced into the flow cell constructed from a HMDS-coated coverslip (*a–c*) or a 300.0-nm-thick Au-coated coverslip (*d–f*). (*a* and *d*) Images of actin filaments infused just after S1 was introduced under rigor conditions. (*b* and *e*) Images of actin filaments infused under the rigor condition after overnight incubation of S1 in the flow cell. (*c* and *f*) *b* and *e*, respectively, after the infusion of the high-salt solution containing ATP (0.6 M KCl, 25 mM imidazole HCl (pH 7.4), 4 mM $MgCl_2$, 1 mM EGTA, 10 mM DTT, and 1 mM ATP). In each preparation, 0.5 mg/ml BSA was infused before the introduction of actin filaments. Temperature, 27 ± 1°C. Scale bar, 10 μm. The BSA was infused into the cell to coat the bare surface to prevent the direct attachment of actin filaments to the surface.

substrate, because all of the atomic coordinates of S1 have not yet been published.

Interaction of actin filaments with S1 adsorbed on a gold surface

We examined the effects of Au-S bond formation on the physiological function of S1 by observing the interaction between the adsorbed S1 molecules and actin filaments. Although almost all actin filaments attached to the surface of the HMDS-coated glass surface (Fig. 7 *a*), none of them attached to the Au-coated glass surface (Fig. 7 *d*) under rigor conditions when the incubation time of S1 molecules was short. After overnight incubation of S1 solution, the extent of actin filaments attached to the Au-coated surface became similar to that of actin filaments attached to the HMDS-coated surface (Fig. 7, *b* and *e*). This indicates that the rate of attachment of the SH groups of S1 molecules on

the gold surface is very slow. This slow attachment was confirmed by the gradual increase in the population of attached S1 molecules (labeled with ^{125}I) (data not shown).

We examined the enzymatic activity of S1 molecules that attached to the gold surface by observing the motility of actin filaments and observing their detachment induced by the addition of high-salt solutions containing ATP. The actin filaments that attached to the gold surface on which S1 molecules had been incubated overnight in advance (Fig. 7 *e*) moved with the same velocity (about 2 μm/s) as that on the HMDS-coated surface. When a high-salt ATP solution was infused, as shown in Fig. 7, *c* and *f*, almost all of the actin filaments detached from both surfaces. Therefore, we conclude that the S1 molecules on the gold surface retain their enzymatic functions to an extent similar to that of S1 molecules on the HMDS-coated surface.

CONCLUSION

We could obtain structural and functional data concerning the monolayer array of the radioactively labeled S1 molecules on the Au substrate in an aqueous solution by analyzing the interference pattern from the radioisotopes and by using an in vitro motility assay. First, the orientation of the adsorbed S1 molecules could be determined from structural data. The IPR method thus makes it possible to obtain structural information about proteins adsorbed on a metal substrate, from a simple analysis of the interference fringes.

The advantage of the IPR method is not only that the instrumentation itself is simple, but also that the experimental analysis can be made under wet conditions without preparing single-crystal samples and without using outer primary beams. We also confirmed that the motor function of the S1 molecules is maintained when they are attached to a gold substrate. If the structural changes of the protein monolayer are synchronized with the enzymatic activity, they must be observed as the vertical movement of the position of radioactive atoms incorporated into a specific site of the protein molecules and as the changes in the total thickness of protein monolayer. In the present work we characterized the S1 monolayer on a gold surface under rigor conditions. The S1 monolayer should also be characterized in the presence of ATP and during its interaction with actin filaments.

Furthermore, we should mention that the binding reaction between Au surface and cysteine residue in the protein is stable. If cysteine residue is mutationally introduced into the outside of the protein as we like, we can control the orientation and characterization of the mutant proteins. In other fields, for example, this new covalent technique between colloidal gold probes and cysteine residue in the protein may also be useful for producing high-resolution labels that are visible in an electron microscope.

REFERENCES

Bolton, A. E., and W. M. Hunter. 1973. The labeling of proteins to high specific radioactivities by conjugation to a ^{125}I-containing acylating agent. *Biochem. J.* 133:529–539.

Caffrey, M., and J. Wang. 1995. Membrane-structure studies using x-ray standing waves. *Annu. Rev. Biophys. Biomol. Struct.* 24:351–377.

Chiang, C., H. Ishida, and J. L. Koenig. 1980. The structure of *g*-aminopropyltriethoxysilane on glass surfaces. *J. Colloid Interface Sci.* 74:396–404

Emoto, Y., T. Kawamura, and K. Tawada. 1985. Characterization of the ATPase active site in myosin subfragment-1 with the use of vanadate plus ADP as a reversible "affinity-labeling" reagent: evidence for heterogeneity in the active sites. *J. Biochem.* 98:351–377.

Hallmark, V. M., S. Chiang, J. F. Rabolt, J. D. Swalen, and R. J. Wilson. 1987. Observation of atomic corrugation on Au(111) by scanning tunneling microscopy. *Phys. Rev. Lett.* 59:2879–2882.

Harada, Y., K. Sakurada, T. Aoki, D. D. Thomas, and T. Yanagida. 1990. Mechanochemical coupling in actomyosin energy transduction studied by in vitro movement assay. *J. Mol. Biol.* 216:49–68.

Itakura, S., H. Yamakawa, Y. Y. Toyoshima, A. Ishijima, T. Kojima, Y. Harada, T. Yanagida, T. Wakabayashi, and K. Sutoh. 1993. Force-generating domain of myosin motor. *Biochem. Biophys. Res. Commun.* 196:1504–1510.

Kinosita, K. Jr., S. Ishiwata, H. Yoshimura, H. Asai, and A. Ikegami. 1984. Submicrosecond, and microsecond rotational motions of myosin head in solution, and in myosin synthetic filaments as revealed by time-resolved optical anisotropy decay measurements. *Biochemistry.* 23:5963–5974.

Kron, S. J., Y. Y. Toyoshima, T. Q. P. Uyeda, and J. A. Spudich. 1991. Assays for actin sliding movement over myosin-coated surfaces. *Methods Enzymol.* 196:399–416.

Moses, P. R., L. M. Wier, J. C. Lennox, H. O. Finklea, J. R. Lenhard, and R. W. Murray. 1978. X-ray photoelectron spectroscopy of alkylamine-silanes bound to metal oxide elctrodes. *Anal. Chem.* 50:576–585.

Muller, W., H. Ringsdorf, E. Rump, G. Wildburg, X. Zhang, L. Angermaier, W. Knoll, M. Liley, and J. Spinke. 1993. Attempts to mimic docking processes of the immune system: recognition-induced formation of protein multilayers. *Science.* 262:1706–1708.

Nishizaka, T., H. Miyata, H. Yoshikawa, S. Ishiwata, and K. Kinosita, Jr. 1995. Unbinding force of a single motor molecule of muscle measured using optical tweezers. *Nature.* 377:251–254.

Rayment, I., W. R. Rypniewski, K. Schmidt-Base, R. Smith, D. R. Tomchick, M. M. Benning, D. A. Winkelmann, G. Wesenberg, and H. M. Holden. 1993. The three-dimensional structure of myosin subfragment-1: a molecular motor. *Science.* 261:50–58.

Sasaki, Y. C., Y. Suzuki, and T. Ishibashi. 1994a. Fluorescent x-ray interference from a protein monolayer. *Science.* 263:62–64.

Sasaki, Y. C., Y. Suzuki, T. Ishibashi, and I. Satoh. 1995. Interference effect of electron-capture x-rays from an ^{125}I-labeled protein monolayer in an aqueous solution. *Anal. Sci.* 11:545–548.

Sasaki, Y. C., Y. Suzuki, Y. Tomioka, and A. Fukuhara. 1993. Observation of an interference effect for fluorescent x-rays. *Phys. Rev. B.* 48: 7724–7726.

Sasaki, Y. C., Y. Suzuki, Y. Tomioka, and T. Ishibashi. 1994b. Site determination of radioactive atoms from the interference effect of electron-capture x-rays. *Phys. Rev. B.* 50:15516–15518.

Suzuki, N., H. Miyata, S. Ishiwata, and K. Kinosita. Jr. 1996. Preparation of bead-tailed actin filaments: estimation of the torque produced by the sliding force in an in vitro motility assay. *Biophys. J.* 70:401–408.

Wagner, P. D. 1982. Preparation and fractionation of myosin light chains and exchange of the essential light chains. *Methods Enzymol.* 85:72–81.

Whitesides, G. M., and P. E. Laibinis. 1990. Wet chemical approaches to the characterization of organic surfaces: self-assembled monolayers, wetting, and the physical-organic chemistry of the solid-liquid interface. *Langmuir.* 6:87–96.